IrrMap: A Large-Scale Comprehensive Dataset for Irrigation Method Mapping

Nibir Chandra Mandal*
Oishee Bintey Hoque*
wyr6fx@virginia.edu
gza5rdr@virginia.edu
University of Virginia
Charlottesville, Virginia, USA

Abhijin Adiga
Biocomplexity Institute,
University of Virginia
Charlottesville, Virginia, USA
abhijin@virginia.edu

Samarth Swarup
Biocomplexity Institute,
University of Virginia
Charlottesville, Virginia, USA
swarup@virginia.edu

Mandy Wilson
Biocomplexity Institute,
University of Virginia
Charlottesville, Virginia, USA
alw4ey@virginia.edu

Lu Feng
University of Virginia
Charlottesville, Virginia, USA
lu.feng@virginia.edu

Yangfeng Ji
University of Virginia
Charlottesville, Virginia, USA
yj3fs@virginia.edu

Miaomiao Zhang
University of Virginia
Charlottesville, Virginia, USA
mz8rr@virginia.edu

Geoffrey Fox
Biocomplexity Institute,
University of Virginia
Charlottesville, Virginia, USA
gcfexchange@gmail.com

Madhav Marathe
Biocomplexity Institute,
University of Virginia
Charlottesville, Virginia, USA
marathe@virginia.edu

arXiv:2505.08273v1 [cs.CV] 13 May 2025

Abstract

We introduce IrrMap, the first large-scale dataset (1.1 million patches) for irrigation method mapping across regions. IrrMap consists of multi-resolution satellite imagery from LandSat and Sentinel, along with key auxiliary data such as crop type, land use, and vegetation indices. The dataset spans 1,687,899 farms and 14,117,330 acres across multiple western U.S. states from 2013 to 2023, providing a rich and diverse foundation for irrigation analysis and ensuring geospatial alignment and quality control. The dataset is ML-ready, with standardized 224×224 GeoTIFF patches, the multiple input modalities, carefully chosen train-test-split data, and accompanying dataloaders for seamless deep learning model training and benchmarking in irrigation mapping. The dataset is also accompanied by a complete pipeline for dataset generation, enabling researchers to extend IrrMap to new regions for irrigation data collection or adapt it with minimal effort for other similar applications in agricultural and geospatial analysis. We also analyze the irrigation method distribution across crop groups, spatial irrigation patterns (using Shannon diversity indices), and irrigated area variations for both LandSat and Sentinel, providing insights into regional and resolution-based differences. To promote further exploration, we openly release IrrMap, along with the derived datasets, benchmark models, and pipeline code, through a GitHub repository: *https://github.com/Nibir088/IrrMap* and Data repository: *https://huggingface.co/Nibir/IrrMap*, providing comprehensive documentation and implementation details.

CCS Concepts

• **Do Not Use This Code → Generate the Correct Terms for Your Paper**.

Keywords

Remote Sensing, Irrigation Mapping, Machine Learning, Multi-modal, Multi-resolution, Satellite Imagery

ACM Reference Format:
Nibir Chandra Mandal, Oishee Bintey Hoque, Abhijin Adiga, Samarth Swarup, Mandy Wilson, Lu Feng, Yangfeng Ji, Miaomiao Zhang, Geoffrey Fox, and Madhav Marathe. 2025. IrrMap: A Large-Scale Comprehensive Dataset for Irrigation Method Mapping . In . ACM, New York, NY, USA, 15 pages. https://doi.org/10.1145/nnnnnnn.nnnnnnn

1 Introduction

Global freshwater demand has increased six-fold over the past century and continues to increase at a rate of 1% per year [45, 60]. Irrigation accounts for 70% of freshwater withdrawals and 90% of consumptive water use worldwide [18, 49, 63]. One of the main factors influencing water availability in irrigated areas is the method of on-farm irrigation used [25, 32]. For instance, widely used surface irrigation technologies (such as flood or furrow irrigation) pose challenges related to irrigation efficiency and downstream water quality, whereas sprinkler systems are often more efficient and less harmful to downstream water quality but require high initial investments, limiting their widespread adoption. Given that irrigated farmland is declining in the western United States as

*Both authors contributed equally to this research.

Permission to make digital or hard copies of all or part of this work for personal or classroom use is granted without fee provided that copies are not made or distributed for profit or commercial advantage and that copies bear this notice and the full citation on the first page. Copyrights for components of this work owned by others than the author(s) must be honored. Abstracting with credit is permitted. To copy otherwise, or republish, to post on servers or to redistribute to lists, requires prior specific permission and/or a fee. Request permissions from permissions@acm.org.

KDD'25, Toronto, ON, Canada

© 2025 Copyright held by the owner/author(s). Publication rights licensed to ACM.

ACM ISBN 978-x-xxxx-xxxx-x/YYYY/MM
https://doi.org/10.1145/nnnnnnn.nnnnnnn

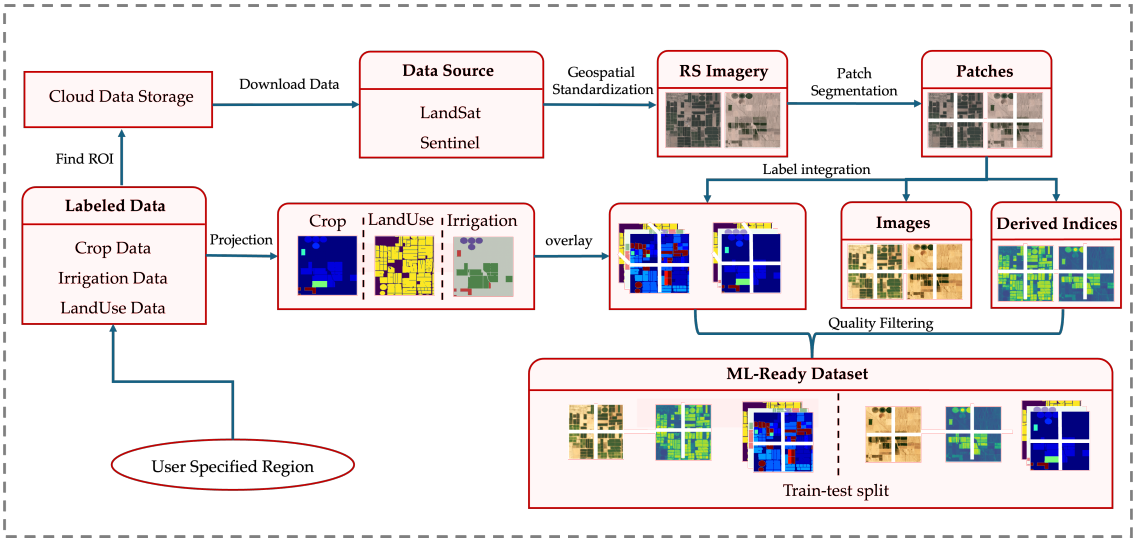

Figure 1: Pipeline for IrrMap dataset acquisition and preparation.

surface water supplies dry up and competition for water from urban, industrial, and environmental sectors intensifies [16, 37], accurate irrigation method identification is crucial for monitoring irrigation patterns and sustainable water resource allocation, particularly in the western United States.

Deep learning (DL) with remote sensing has shown significant potential in various geospatial agricultural mapping tasks [28, 61], such as crop classification [14, 40, 41], farm boundary detection, farm infrastructure detection, and species mapping [1, 7, 22, 24, 27, 30]. However, its application in irrigation method classification remains limited due to the absence of a large-scale ML-ready irrigation method dataset. Existing datasets like LANID and IrrMapper provide 30-meter resolution maps but only distinguish between irrigated and non-irrigated lands without differentiating irrigation methods [29, 62].

Creating a large-scale irrigation dataset across different regions is particularly challenging. Firstly, there is no centralized database; data for different states in the US can potentially come from different sources. Therefore, we see variations in classification systems, spatial resolutions, and labeling standards of different agencies. For instance, what is classified as "Center Pivot" irrigation in Arizona may be labeled as "Big Gun" irrigation in Washington, which requires a systematic approach to ensure consistent labeling across the region. Moreover, significant variation in farm sizes poses a challenge in balancing high-resolution mapping for small farms while ensuring comprehensive regional coverage. Textural patterns of irrigation type could be heavily influenced by crop type, soil, etc. Additional contextual information, such as crop types and vegetation indices, can be beneficial to improve classification accuracy [2, 13].

1.1 Our Contributions

In this work, we introduce IrrMap, a large-scale comprehensive dataset for irrigation mapping designed to (*i*) support the development of machine learning (ML) models that identify various irrigation methods, and (*ii*) accelerate mapping various agricultural infrastructure to support resilience in food systems and water availability. Our dataset includes satellite imagery along with key variables relevant to irrigation mapping, such as crop type, land use data, and derived vegetation indices. It spans multiple states across the U.S., covering 1,668,899 farms and 11,443,492 acres from 2013 to 2023. To the best of our knowledge, IrrMap is the first and largest dataset dedicated to data-driven irrigation method mapping. As discussed below, our work addresses each of the criteria laid out in the call for paper, namely: (*i*) *Accessibility*: the dataset is public (Huggingface); (*ii*) *Quality and Documentation*: Automated and manual quality checks were conducted, along with documentation of the dataset, pipeline and analysis; (*iii*) *Impact*: The multi-modal dataset and derived models can be extended for national-scale mapping of irrigation and related problems as well as promote methodological advances (outlined in Section 7); (*iv*) *Ethics and Fairness*: Our collected data is based solely on publicly available sources and is provided for research purposes, ensuring transparency and reproducibility

Multi-resolution satellite imagery. To accommodate diverse research needs, we integrate multi-resolution data from LandSat (30m × 30m) and Sentinel (10m × 10m), ensuring a balance between detail and scalability. High-resolution imagery enables fine-grained analysis of irrigation patterns and small-scale variations, while lower-resolution data facilitates large-scale assessments with reduced computational overhead, making it ideal for regional and national studies. Besides, LandSat data is available for more years compared to Sentinel data allowing for more detailed temporal evolution studies of irrigation.

Irrigation method annotation. Since irrigation label data is not centralized, we manually collected mapping data for four states—Arizona (AZ), Colorado (CO), Washington (WA), and Utah (UT)—along with land use and crop layer datasets. These datasets were carefully cleaned and integrated with the imagery.

Agricultural related indices and masks. Additionally, we computed twelve vegetation indices to further enhance the irrigation mapping task. By providing these indices, IrrMap ensures accessibility to researchers beyond remote sensing experts, making it easier for hydrologists, agronomists, and ML practitioners to leverage the dataset without requiring additional domain-specific preprocessing.
ML-ready data processing. Beyond providing data, IrrMap also includes a complete pipeline for generating ML-ready datasets in new regions, eliminating manual efforts for researchers, particularly for irrigation mapping, and with minor modifications for similar applications. Following our pipeline (Figure 1), given a Region of Interest (ROI), LandSat and Sentinel images are downloaded from USGS Earth Explorer[1]. We then process a total of 25.6 TB of large image tiles into high-quality one million 224×224 GeoTIFF patches (6.2 TB), ensuring precise geospatial alignment and rigorous quality control, before combining them with their corresponding labels.
Data analysis. To better understand how crop type influences irrigation type mapping and how irrigation method representation varies across different dataset resolutions, we conduct a preliminary analysis of irrigation method distribution across crop groups and spatial patterns, examining irrigation preferences across geographic regions and variations in irrigation diversity across datasets with different spatial resolutions.
Benchmarking. We also establish benchmarks using deep learning (DL) models trained on different input modalities, including RGB, RGB with Crop Type, RGB with Land Use, and RGB with NDVI, demonstrating their effectiveness in irrigation mapping tasks.
Data availability. To encourage further research and facilitate the development of similar datasets, we openly publish IrrMap, including dataloaders, trained models, benchmark results, and the complete pipeline for dataset generation and training the benchmark models. We also provide a *https://github.com/Nibir088/IrrMap* and Data repository: *https://huggingface.co/Nibir/IrrMap* with comprehensive documentation on dataset usage and model implementation. These resources serve as a valuable reference for expanding irrigation mapping efforts across the globe.

2 Related Work

Current irrigation mapping products provide spatial data without detailed irrigation methods [47, 52]. While remote sensing has been utilized to map irrigated fields, especially in areas of mixed agriculture [3], distinguishing between irrigation types remains challenging due to landscape complexity and subtle practice variations. In addition, existing datasets for irrigation has offered large spatial coverage but lacks high-resolution imagery or often suffer from outdated data [5, 38]. Global Irrigated Area Map (GIAM) [15, 57], Global Map of Irrigation Areas (GMIA) [51], Global Land Cover Characteristics (GLCC) [35], and Global Food-Support Analysis Data (GFSAD) have global spatial coverage for irrigated lands but use one-kilometer resolution [56]. MIrAD (250-meter resolution) relies on census-based estimates, leading to classification error [6, 42]. Although AIM-HPA (30-meter resolution) provides high-resolution irrigation data, its coverage is limited to the High Plains [12]. Recent work on landsat-based irrigation datasets, LANID (30-meter resolution) and IrrMapper, contains irrigated lands without labels for irrigation methods [29, 62].

Deep learning and remote sensing based mapping has been applied recently for various agricultural applications, leveraging satellite and aerial imagery. Some active areas include crop-type and crop-land detection [8, 27, 41]. In the context of livestock agriculture, there have been some works in mapping large farms due to environmental concerns [7] and mixed farming [22]. Farm boundary detection uses segmentation techniques applied to satellite imagery, leveraging edge detection and deep learning models to delineate agricultural plots [9, 64]. Mapping invasive species is another emerging area [1, 14, 30, 40]. Although these datasets provide extensive agricultural monitoring capabilities, large-scale irrigation mapping data remains largely unavailable. The absence of such data hinders efforts to accurately assess water usage, monitor drought impacts, and optimize irrigation efficiency. Given the increasing concerns over water scarcity and sustainable agriculture, comprehensive irrigation mapping would be critical for policymakers, water resource managers, and farmers to implement efficient water allocation strategies.

Computer vision and machine learning have made strides in identifying specific systems like center pivots [11, 46, 48] but the broader task of irrigation mapping demands nuanced analysis. In the western U.S. and other dry regions of the world, a variety of irrigation methods coexist on the landscape. In an irrigated watershed of southern Idaho, Bjorneberg et al. found that the proportion of the agricultural land irrigated with sprinklers increased from 6% in 2006 to 59% in 2016 as furrow irrigated fields were converted to sprinkler systems [4]. Evaluating the effect of different irrigation methods on basin-scale processes requires accurate information on the location and distribution of the types of irrigation used on-farm across the irrigated landscape. Currently available irrigation mapping products [42, 47, 50, 53] distinguish between irrigated and non-irrigated areas at various spatial scales without explicit information on the methods of irrigation. Regional-scale irrigation mapping from remotely sensed data has been the object of many studies [3, 4, 42].

3 Description of Data Source

General Information. Our multi-resolution dataset IrrMap consists of around one million patches containing LandSat and Sentinel imagery. The dataset includes pixel-precise irrigation mapping, land use, and crop cover annotations at both 30m and 10m resolutions while preserving the geolocation of each patch (Table 1). Our dataset covers four states—Arizona, Colorado, Utah, and Washington—spanning approximately 1,443,492.31 acre of U.S. agricultural lands (shown in Figure 2 and Table 2).
Remote Sensing Data Source. LandSat-8 and Sentinel-2A imagery were obtained from USGS Earth Explorer for Utah, Arizona, Washington, and Colorado, covering their respective study periods. LandSat-8 provides 30m multispectral and 100m thermal resolution with a 16-day revisit cycle, while Sentinel-2A offers 10m visible and near-infrared resolution with a 5-day revisit cycle. Data acquisition focused on the irrigation season (March–September), a key period for assessing water use and crop conditions, as imagery from other periods may capture snow cover, bare soil, or dormant

[1]https://earthexplorer.usgs.gov/

Table 1: Summary of spatial and temporal coverage

State	Year Range	Irrigation Type (%)				Area (acres)	#Farms
		Drip	Sprinkler	Flood	Other		
AZ	2013-17	7.84	20.05	45.67	26.43	566,340.14	16,991
CO	2018-20	0.15	40.24	58.59	1.02	2,560,487.77	131,585
UT	2021-23	0.08	34.22	30.60	35.10	2,673,838	794,202
WA	2015-20	1.70	20.41	1.93	75.96	8,316,664.40	726,121
Total	-	1.36	26.60	19.39	52.65	14,117,330.31	1,687,899

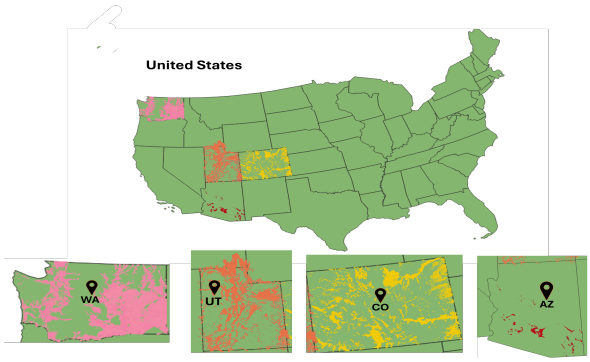

Figure 2: Coverage area of the irrigation method dataset.

Table 2: Overview of the Irrigation Mapping Dataset, including spectral image information from LandSat and Sentinel satellites, along with auxiliary data such as derived indices, irrigation mapping, crop data layers, and land use information.

Data Category	Description	Patch Shape
Spectral Image	LandSat 30m: Coastal (Band 1), Blue (Band 2), Green (Band 3), Red (Band 4), NIR (Band 5), SWIR-1 (Band 6), SWIR-2 (Band 7), Thermal (Band 10 & 11)	224x224x9
	Sentinel 10m: Coastal (Band 1), Blue (Band 2), Green (Band 3), Red (Band 4), Red Edge 1 (Band 5), Red Edge 2 (Band 6), Red Edge 3 (Band 7), NIR (Band 8), SWIR-1 (Band 11), SWIR-2 (Band 12)	224x224x10
Auxiliary Information	Irrigation Map: Other (0), Flood (1), Sprinkler (2), Drip (3)	224x224x4
	Derived Indices: NDVI, EVI, GNDVI, SAVI, MSAVI, RVI, CIgreen, NDWI, PRI, OSAVI, WDRVI, NDTI	224x224x12
	Crop Data: Alalfa, Cereals, Cover Crop, Fibres, Fruits, Grass, Green House, Herb Group, Horticulture, Nursery, Nuts, Oil-bearing Crops, Orchard, Pulses, Roots and Tubers, Shrub Plants, Sugar Crops, Vegetables, Vinetard, Unknown. (One-Hot Encoded, Mapped with Each Patch)	224x224x21
	Land Use: Binary Mask	224x224x1

vegetation, making it less useful for irrigation analysis. Images exceeding 5% cloud cover, snow, or poor quality—identified via the Quality Assessment (QA) band—were excluded.

Irrigation Data Source. Since *irrigation label data* is not readily available from a single source for all states, we collected data for four states from different sources. For Utah (2021–2023), we obtained data from the Water-Related Land Use (WRLU)[2] dataset. Washington's irrigation data (2015–2020) was sourced from the Washington State Department of Agriculture Agricultural Land Use dataset (WSDA)[3], while Colorado's data (2018–2020) was acquired from the Colorado Decision Support System (CDSS)[4], which provides Geographic Information System (GIS) datasets for all river basins. For Arizona (2015–2017), we utilized the USGS Verified Irrigated Agricultural Lands dataset[5], a GIS geodatabase developed collaboratively by USGS and the University of Wisconsin. All of these datasets include various land use details, such as vector polygons of irrigated fields, irrigation methods, crop types, water sources, and acreage information across different years. To standardize the analysis across data sources, we mapped various irrigation practices to three primary methods: drip, sprinkler, and flood irrigation (see Table 4). For example, "Center Pivot", "Wheeler Sprinkler", and "Traveling Gun" all fall under sprinkler irrigation. In addition, some labels are noisy as multiple irrigation methods are assigned to a single entry (e.g., "Drip/Rill/Sprinkler" or "Center Pivot/Drip/Sprinkler"). To maintain clarity, such noisy labels are removed, ensuring clean, structured data for reliable analysis. Irrigation methods vary by state; Utah's 2.7 million acres have 0.08% drip, 34% sprinkler, and 31% flood, while Arizona's 566,340 acres include 8% drip, 46% flood, and 20% sprinkler irrigation (See Table 1).

Crop Data Source. For Crop Data, A total of 143 distinct crop types were identified across the four states from USGS Verified Irrigated Agricultural Lands datasets. To standardize the analysis, we consolidated these crops into 20 categorical groups based on classifications from Leff et al. [31] and definition from the IR4-Project of U.S. Department of Agriculture (USDA) [43]. The groups are: Alfalfa, Cereals, Cover Crop, Fibres, Fruits, Grass, Green House, Herb Group, Horticulture, Nursery, Nuts, Oil-bearing crops, Orchard, Pulses, Roots and Tubers, Shrub Plants, Sugar Crops, Vegetables, Vineyard, and an additional category for unspecified crops. For instance, the cereal group includes barley, corn, wheat, and sorghum, while the fruit group encompasses apples, berries, citrus, and melons. The complete mapping of individual crops to their respective groups is provided in the Appendix Table 10.

[2]https://dwre-utahdnr.opendata.arcgis.com/pages/wrlu-data
[3]https://agr.wa.gov/departments/land-and-water/natural-resources/agricultural-land-use
[4]https://dwr.colorado.gov/services/data-information/gis
[5]https://catalog.data.gov/dataset/verified-irrigated-agricultural-lands-for-the-united-states-200217

Land-Use Data Source. For *Agricultural Land Use Data*, the study area encompasses various land use categories including irrigation, dry agriculture, idle, riparian, sub-irrigation, urban, urban grass, water, and wet flats. From these categories, we focused specifically on irrigated land and agricultural land, as these represent the primary zones requiring active irrigation management.

Table 3: IrriMap Dataset Distribution Across Western U.S. States for Sentinel and LandSat Imagery. The dataset is divided into training and testing splits for machine learning applications.

Source	Split	Regions				IrrMap
		AZ	UT	WA	CO	
LandSat	Train	2,655	40,224	26,852	18,284	88,015
	Test	665	10,057	6,716	4,573	22,011
	Total	**3,320**	**50,281**	**33,568**	**22,857**	**110,026**
Sentinel	Train	7,930	306,767	262,206	269,596	846,499
	Test	1,985	76,693	65,555	67,401	211,634
	Total	**9,915**	**383,460**	**327,761**	**336,997**	**1,058,133**

Table 4: Irrigation Method Mapping

Original Label	Mapped Label
Drip Microirrigation, Micro-Drip, DRIP, Drip	Drip
Traveler Sprinkler, Center Pivot - Tow, Solid State Sprinkler, Overhead, Traveling Gun, Pivot, Traveling Gun, pivot, sprinkler, Center Pivot, Micro-Sprinkler, Micro-Bubbler, Mirco-Bubbler, Sprinkler & Bubbler, Lateral, Side Roll, Lateral Sprinkler, Other Sprinkler, Microsprinkler, Big Gun, Wheel Line, Big Gun/Sprinkler, Sprinkler/Wheel Line, Big Gun/Center Pivot, Center Pivot/Sprinkler, Center Pivot/Wheel Line, Center Pivot/Sprinkler/Wheel Line, Big Gun/Wheel Line, Wheel line, SPRINKLER, Sprinkler	Sprinkler
Furrow, Grated_Pipe, Improved Flood, Rill, Hand/Rill, None/Rill, Grated_pipe, Gated_pipe, FLOOD, FURROW, GATED_PIPE	Flood
Not Specified, Micro, No Label, Research, Uncertain, Drip/None, Hand, Big Gun/Drip, Drip/Big Gun, Drip/Rill/Sprinkler, Rill/Sprinkler, Drip/Micro-Sprinkler, Drip/Wheel Line, Center Pivot/Rill, Rill/Wheel Line, Drip/Rill, Center Pivot/None, Center Pivot/Rill/Wheel Line, Center Pivot/Rill/Sprinkler, Rill/Sprinkler/Wheel Line, Center Pivot/Drip, Hand/Sprinkler, Drip/Sprinkler, Sub-irrigated, Dry Crop, Sprinkler And Drip, Center Pivot/Drip/Sprinkler, None/Sprinkler/Wheel Line, Unknown	Removed

4 ML-ready Dataset Preparation

We create a structured (consistent formats, encoded categorical values, and normalized numerical data) and preprocessed (spatially consistent, quality-checked, feature engineered, and carefully partitioned into train/test) ML-ready dataset (IrrMap) for seamless application of ML models as follows:

Complete Data Processing Pipeline. To streamline the dataset preparation process, we developed a pipeline that performs preprocessing, patch segmentation, label integration, and train-test splitting as shown in Figure 1. Through this pipeline, we have streamlined **25.61 TB** of raw satellite data into a well-structured **6.2 TB** IrrMap dataset, significantly enhancing accessibility and usability of the dataset. The entire pipeline is built using GDAL, Rasterio, OpenCV, and PyTorch Lightning, ensuring efficiency and reproducibility. In addition, we provide a PyTorch Lightning DataModule that allows seamless integration with deep learning models. Now, we describe each step of the pipeline.

Data acquisition. We acquired 2,407 and 36,638 image tiles from LandSat and Sentinel respectively, totaling 25.61 TB (2.78 TB for LandSat and 22.83 TB for Sentinel) of data and covering over 11 million acres of irrigated land in the western United States.

Geospatial Standardization. We first reproject each LandSat and Sentinel image to the WGS-84/EPSG:4326 coordinate system to ensure uniformity across the collected satellite images from different regions [54]. This facilitates accurate overlaying with ground truth label from different sources (e.g., crop labels, irrigation labels, land use labels, etc.).

Patch Segmentation. Following standard practices, we divide each image into 224×224 non-overlapping patches to reduce computational complexity while maintaining spatial integrity. Each patch covers approximately 45 square kilometers at 30m resolution for LandSat and 5 square kilometers at 10m resolution for Sentinel, ensuring a balance between capturing relevant spatial information and offering efficient deep learning model training. Moreover, we discard all patches containing poor-quality pixels to ensure data quality and reliability (based on QA-Bands).

RGB Images Creation. We extract the Red, Green, and Blue bands from satellite imagery (e.g., LandSat or Sentinel) and stack ($224 \times 224 \times 3$) them to form a true-color composite. In addition, we apply the standard step of gamma correction (a nonlinear adjustment) that modifies image brightness and contrast by altering pixel intensity values for improved visibility [44]).

Derived Indices Creation. To enhance surface property analysis for irrigation mapping, we compute various spectral indices capturing vegetation health[6], soil conditions, and water availability. NDVI, GNDVI, and CIgreen assess vegetation vigor and chlorophyll content, while EVI, SAVI, and MSAVI adjust for atmospheric and soil background effects, improving vegetation monitoring in different environments [23, 39, 59]. NDWI detects water bodies and moisture content, aiding in drought assessment, whereas NDTI distinguishes tilled from untilled soils for land management analysis [19, 65]. PRI measures plant stress and photosynthetic efficiency, OSAVI refines soil adjustment for vegetation detection, and WDRVI enhances differentiation in high biomass areas [17, 20, 58]. RVI provides an alternative vegetation measure with reduced sensitivity to atmospheric variations [21]. Together, these indices offer valuable insights for irrigation mapping, agricultural monitoring, and environmental assessment (More details in Appendix Table 9).

[6] https://www.nv5geospatialsoftware.com/docs/AlphabeticalListSpectralIndices.html

Label Integration. We begin by projecting all label data, including crop, irrigation, and land use information, into the WGS-84 coordinate system (EPSG:4326) to ensure accurate spatial alignment with our satellite image patches. A pixel-wise labeling approach is then employed to integrate these labels into a unified structure. This structured integration enables a precise and consistent representation of irrigation, crop type, and land use information while ensuring data reliability and spatial coherence.

- **Irrigation Mask.** Each patch is assigned an irrigation mask $Y \in \{0, 1, 2, 3\}^{224\times224}$, where each pixel is mapped to one of four irrigation methods: 0 (Others/No-Irrigation), 1 (Flood), 2 (Sprinkler), and 3 (Drip).
- **Crop Mask.** We generate a crop mask $C \in \{0, 1, \ldots, 21\}^{224\times224}$, where each pixel is classified into one of 21 crop types, with 0 indicating no crop presence.
- **Land Mask.** A binary land mask, $L \in \{0, 1\}^{224\times224}$, is derived from land use data, where 1 represents agricultural land and 0 denotes non-agricultural areas, ensuring spatial integrity.

Quality Filtering. Since the majority of created patches lack valid irrigation data, we exclude patches where more than 99.99% of pixels are labeled as non-irrigated. This ensures that each selected patch contains meaningful irrigation information for analysis. After quality filtering, we find a total of 110,026 patches for LandSat imagery and 1,058,133 patches for Sentinel (shown in Table 3). Even after following standard filtering processes to filter imagery affected by snow, clouds, or shadows (as guided by the data quality band), there were issues with several images (see Appendix Figure 6). We had to manually verify and annotate more than 18,000 patches to resolve this issue. Each patch in our dataset is assigned a binary data quality label$Q \in \{0, 1\}$, where 0 indicates contamination due to clouds, shadows, or snow and 1 represents a clean image. This ensures that only high-quality patches are retained for model training.

Train-Test Splitting. To ensure a robust and unbiased evaluation of machine learning models, we carefully split the IrriMap dataset into 80% training and 20% testing sets. As irrigation practices vary significantly vary across different geographical regions (e.g., Utah has only 0.08% drip-irrigated lands in the labeled data), a state-wise stratified split is performed. Each state's dataset is independently divided into an 80-20% split, and the resulting 20% testing portions are then combined to form a spatially well-represented test set, thereby mitigating geographic biases. State-wise distribution of training and testing datasets is shown in Table 3. A total of 934,514 (88,015 for LandSat and 846,499 for Sentinel) patches are created for the training dataset. The test dataset has 233,645 (22,011 for LandSat and 211,634 for Sentinel) patches in total.

5 Data Analysis

Irrigation-Crop Relationship. Our analysis of irrigation methods across farms highlights distinct preferences based on crop groups in Figure 3. We notice that vineyards rely on drip irrigation only, while nursery and orchard farms generally use drip irrigation. This analysis emphasizes the need for precise water control in high-value crops. Fruit and root crops are mainly irrigated using sprinkler systems, which provide uniform water distribution, whereas fiber crops, such as cotton, depend heavily on flood irrigation. Notably, greenhouse farms avoid flood irrigation and opt for more controlled sprinkler and drip methods, while shrub plant farms do not use sprinkler irrigation. These findings underscore the relationship between the crop types and irrigation methods.

Irrigation Diversity. To understand the diversity of irrigation practices within the dataset, we quantify diversity using Shannon Index [36]. For each patch, we calculate the Shannon diversity index H for each patch as follows:

$$H = -\sum_i \frac{p_i}{\sum_j p_j} \times \ln\left(\frac{p_i}{\sum_j p_j}\right) \tag{1}$$

which p_i represents the fraction of area occupied by the irrigation method i and $i, j \in \{\text{Drip, Sprinkler, Flood}\}$. If a patch contains only one irrigation method, the Shannon index is 0 (indicates homogeneous), whereas a patch with mixed irrigation has a higher diversity score. Note that the score is highest when all three (drip, sprinkler, and flood) have equally irrigated lands within the patch.

The varying complexity of irrigation mapping in the dataset is evident in the Shannon diversity indices of our dataset patches (as shown in Figure 4). We notice that the IrrMap dataset (both LandSat and Sentinel) have similar pattern, with a high concentration of low-diversity patches and a secondary peak near 0.7 (indicates diverse irrigation practices). We further show that a significant portion of the dataset consists of homoegeneous patches (42,615 for LandSat and 492,821 for Sentinel) where a single irrigation method is only available within the patch. However, LandSat data has 48% homogeneous patches compared to 58% of homogeneous patches for Sentinel, suggesting a higher representation of diversely irrigated lands for LanSat. As Sentinel captures 10-meter-resolution images, the patches zoom into the farmlands and provide finer spatial details. This leads to a higher proportion of homogeneous patches. In contrast, LandSat patches cover a broder area (45 km^2 per patch), capturing multiple irrigation methods within a patch. It is worth noting that patches from Sentinel provide finer details with low coverage, leading to increased training and evaluation costs, whereas LandSat patches cover more area with higher diversity, leading to challenges for correctly identifying irrigation methods from a machine learning perspective.

6 Benchmarking

To evaluate the effectiveness of IrrMap for irrigation method classification, we designed an experiment using satellite imagery from Landsat. Our goal is to classify irrigation types—Flood, Sprinkler, and Drip—by leveraging different input modalities and benchmarking their performance across various configurations. We employed a UNet-style ResNet-34 architecture for all baseline experiments, training the models on the complete Landsat training dataset and presenting results on the test set of each state. We train the model for 10 epochs on an NVIDIA A100 80GB GPU. The motivation behind this experiment is to assess how incorporating auxiliary modalities—such as NDVI, Crop Mask, and Land Mask—alongside RGB imagery improves impact the performance. More hyper-parameter settings and results on the Sentinel data are present in Appendix D Table 8.

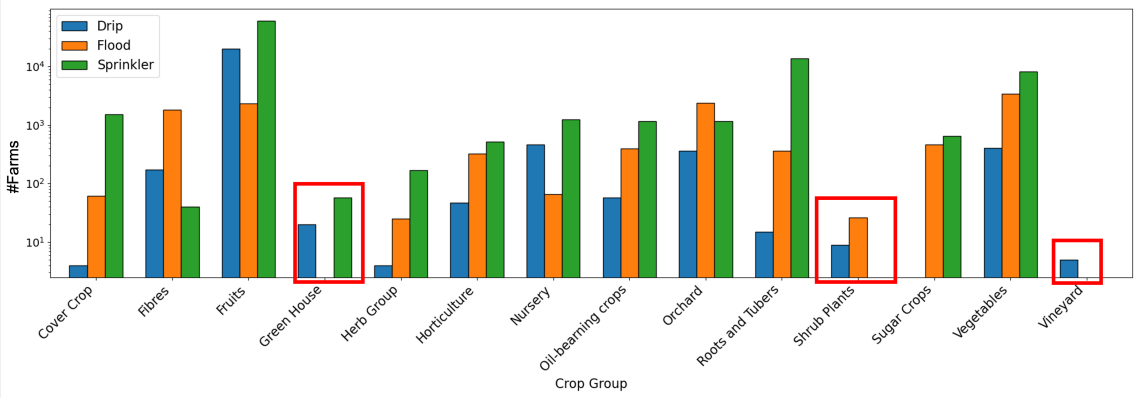

Figure 3: Distribution of irrigation methods (Drip, Flood, and Sprinkler) across different crop groups for the studied regions. Y-axis denotes the number of farms in log-scale. Some crop groups, such as 'Green House' and 'Vineyard' do not use flood irrigation, whereas 'Shrub Plants' cultivated farms do not use sprinkler irrigation. Noteably, 'Nursery' and 'Fruit' cultivated farms prefer drip irrigation more than flood irrigation. Sprinkler irrigation is popular in 'Root and Tube' cultivated farms across the studied regions.

Table 5: Irrigation Classification Performance for Different Modalities, reporting Precision (P), Recall (R), F1-score (F), and Intersection over Union (IoU) for Flood, Sprinkler, and Drip irrigation types across different states. More results on Sentinel data are in Appendix D Table 8.

State	Modality	Flood				Sprinkler				Drip			
		P	R	F	IoU	P	R	F	IoU	P	R	F	IoU
AZ	RGB	0.5937	0.4673	0.5230	0.3541	0.5744	0.4247	0.4883	0.3231	0.4744	0.3604	0.4096	0.2576
	RGB+CROP	**0.7359**	**0.8093**	**0.7708**	**0.6271**	**0.7070**	**0.7473**	**0.7266**	**0.5706**	**0.6821**	**0.6306**	**0.6554**	**0.4874**
	RGB+LAND	0.6589	0.7588	0.7054	0.5448	0.6700	0.6628	0.6664	0.4997	0.6744	0.4089	0.5091	0.3415
	RGB+NDVI	0.5966	0.5653	0.5805	0.4090	0.6288	0.4016	0.4901	0.3246	0.4745	0.3977	0.4327	0.2761
CO	RGB	0.6108	0.2555	0.3603	0.2197	0.5857	0.4111	0.4831	0.3185	0.0000	0.0000	0.0000	0.0000
	RGB+CROP	**0.6909**	**0.6477**	**0.6686**	**0.5022**	**0.7251**	**0.6695**	**0.6962**	**0.5340**	**0.2798**	**0.1653**	**0.2078**	**0.1159**
	RGB+LAND	0.6648	0.5497	0.6018	0.4304	0.6701	0.5926	0.6290	0.4588	0.2659	0.0239	0.0438	0.0224
	RGB+NDVI	0.5660	0.3979	0.4673	0.3049	0.6415	0.3752	0.4734	0.3101	0.0000	0.0000	0.0000	0.0000
UT	RGB	0.6215	0.3030	0.4074	0.2558	0.5307	0.5341	0.5324	0.3628	0.0000	0.0000	0.0000	0.0000
	RGB+CROP	**0.6741**	**0.6549**	**0.6644**	**0.4974**	**0.6870**	**0.7138**	**0.7001**	**0.5386**	**0.4221**	**0.0139**	**0.0269**	**0.0136**
	RGB+LAND	0.6878	0.6427	0.6645	0.4976	0.6746	0.6579	0.6661	0.4994	0.1530	0.0028	0.0055	0.0028
	RGB+NDVI	0.5909	0.4135	0.4866	0.3215	0.5927	0.4598	0.5179	0.3494	0.0000	0.0000	0.0000	0.0000
WA	RGB	0.4503	0.1304	0.2023	0.1125	0.5693	0.4607	0.5093	0.3416	0.3766	0.0949	0.1516	0.0820
	RGB+CROP	**0.5926**	**0.4548**	**0.5146**	**0.3464**	**0.7237**	**0.7725**	**0.7473**	**0.5966**	**0.4899**	**0.5068**	**0.4982**	**0.3317**
	RGB+LAND	0.5256	0.4264	0.4709	0.3079	0.7013	0.7316	0.7161	0.5577	0.5283	0.3326	0.4082	0.2564
	RGB+NDVI	0.3794	0.2458	0.2983	0.1753	0.5872	0.4490	0.5089	0.3413	0.4147	0.1238	0.1907	0.1054

The results demonstrate that incorporating additional feature layers alongside RGB imagery leads to varying degrees of improvement in irrigation classification performance. RGB + Crop Mask consistently achieves the highest accuracy, with an average F1-score improvement of 30–50% over RGB alone, particularly excelling in Flood and Sprinkler irrigation. The Land Mask augmentation also enhances classification, yielding a 20–40% increase in IoU and F1-score compared to RGB-only, especially for Flood irrigation. Meanwhile, NDVI augmentation provides moderate benefits, with a 10–25% boost in F1-score and IoU for Sprinkler and Flood irrigation methods but does not perform as well for Drip irrigation. RGB-only models still produce reasonable results, particularly for Flood irrigation, but exhibit relatively lower performance in distinguishing Sprinkler and Drip irrigation methods. These findings suggest that crop-specific information (via Crop Mask) is the most informative additional layer, while land use and vegetation indices (NDVI) contribute moderately, depending on the irrigation methods. This opens up an interesting research direction on how to

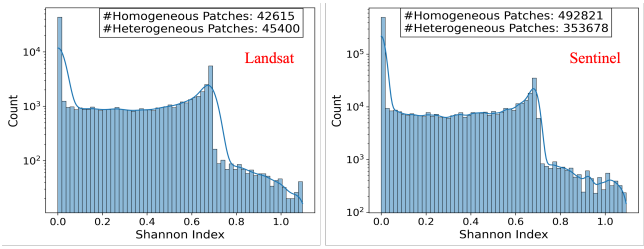

Figure 4: The figure shows irrigation patterns for the IrrMap dataset through Shannon diversity indices. The left figure presents the distribution for the LandSat data, whereas the right figure displays for the Sentinel data. Two distinct spatial patterns are noticed: both single-method dominance in some patches and mixed irrigation practices (index 0.6) in others.

best leverage these additional modalities—whether through feature fusion techniques, advanced model architectures, or task-specific weighting—to achieve optimal performance.

7 Potential Applications of the Dataset

In addition to irrigation mapping, our IrrMap dataset has a wide range of agricultural applications, as follows:

- **Homogenous and Heterogenous Irrigated Field Identification**: Our large-scale dataset enables classifying irrigation patterns into homogeneous (single practice) and heterogeneous (mixed practice) regions, improving water resource analysis. Additionally, 20K labeled samples of cloud, snow, and shadow enhance quality control models for filtering contaminated satellite imagery, ensuring reliable agricultural monitoring.
- **Temporal Pattern Recognition and Change Detection in Irrigation Over Years**: A trained model using IrrMap, can be used for hindcasting, analyzing past irrigation practices, crop distribution, and land-use changes. By leveraging historical satellite imagery and spectral indices, the model can detect shifts in irrigation methods, variations in soil moisture, and crop rotation patterns. This enables researchers to assess long-term trends in water usage and agricultural adaptation.
- **Foundation Model for Agricultural Assets**: The large-scale nature of our dataset provides an opportunity to build foundation models for agricultural applications [10, 26, 55]. The dataset can be used to develop agricultural-specific foundation models through self-supervised pretraining, enabling transfer learning for regions with limited labeled data. Clustering algorithms can identify similar agricultural practices across different regions, while anomaly detection systems can spot unusual irrigation practices.
- **Irrigation Mapping through Knowledge-Guided Deep Learning**: Beyond pure machine learning approaches, our dataset supports the development of hybrid systems that combine agricultural domain knowledge with data-driven insights [33, 34]. These models can integrate expert knowledge about crop information, local agricultural practices, and regional climate patterns with machine learning predictions to provide more reliable and practical solutions. Applications include smart irrigation scheduling systems that consider multiple factors (crop type, growth stage, irrigation practice, weather patterns), resource optimization tools for water, and decision support systems for crop rotation planning.

In addition, our proposed pipeline (Figure 1) streamlines the collection, processing, and integration of multi-scale satellite data, significantly reducing the effort required for large-scale geospatial analysis. By leveraging labeled shapefiles, it queries and retrieves satellite imagery (Sentinel and LandSat) from cloud platforms such as Earth Explorer (EE). The pipeline also automates spatial patch generation, seamlessly aligning satellite imagery with auxiliary datasets like climate analysis models and soil structure maps.

8 Limitation of the dataset

The IrriMap dataset and trained model are currently limited to the western United States, which may restrict its applicability to regions with different climatic and agricultural conditions. All collected irrigation mapping data sources assume that irrigation practices and crop cultivation remain consistent throughout a season, which may not account for intra-seasonal variations due to environmental or management changes. Additionally, since the dataset is merged from multiple sources, it is subject to data inconsistencies, noise, and rasterization artifacts that may impact accuracy. Moreover, during the irrigation mapping, we drop the irrigated lands that have multiple or ambiguous irrigation labels. Furthermore, cropland data is generated through modeling, making it important not to over-rely on it for absolute ground truth. Groundwater data is not available in our IrrMap, limiting the model's ability to assess subsurface water interactions.

9 Conclusion

We present IrrMap, a large-scale ML-ready dataset (1.1 million patches) for irrigation mapping by combining multi-resolution satellite imagery with crop, land use, and vegetation indices that covers 14.1 million acres of farmland. The dataset provides a comprehensive view of irrigation method distribution, spatial diversity, and crop-irrigation relationship. Our benchmark results demonstrate that incorporating auxiliary data such as crop, land use, and vegetable indices significantly improves irrigation classification accuracy. Moreover, our pipeline for ML-ready datasets is designed for data integration that enables seamless incorporation of additional data layers to expand analytical capabilities.

In future work, we plan to expand IrrMap to diverse agricultural regions, particularly semi-arid and developing agricultural landscapes. We aim to integrate temporal analysis using historical and near-real-time satellite imagery to track shifts in irrigation adoption and drought monitoring. In addition, incorporating groundwater data, soil moisture estimates, and real-time climate variables would enable holistic and precise irrigation monitoring, supporting sustainable water resource management.

Acknowledgments

This material is based upon work supported by the AI Research Institutes program supported by NSF and USDA-NIFA under the AI Institute: Agricultural AI for Transforming Workforce and Decision Support (AgAID) award No. 2021-67021-35344.

References

[1] Aniruddha Adiga, Surbhi Singh, Ethan Choo, Johnny Yang, Srinivasan Venkatramanan, Anjana Devkota, Bharat Babu Shrestha, Seerjana Maharjan, Sita Gyawali, Sandeep Dhakal, Krishna Poudel, Pramod Kumar Jha, Rangaswamy Muniappan, Madhav Marathe, and Abhijin Adiga. 2023. A Robust Deep Learning Framework Reveals the Spread of Multiple Invasive Plants in a Biodiversity Hotspot using Satellite Imagery. In *The Workshop on Artificial Intelligence for Social Good (in AAAI)*.

[2] L. Niel Allen, Alfonso Torres-Rua, Anastasia Thayer Hassett, Ryan Larsen, and Matt Yost. 2021. *Utah Agricultural Water Optimization - Water Savings from Drip Irrigation.* Technical Report. Utah State University. https://water.utah.gov/wp-content/uploads/2021/12/Utah-Ag-Water-Optimization-Drip-Irr-USU-Dec-2021.pdf

[3] H. Bazzi, N. Baghdadi, D. Ienco, M. El Hajj, M. Zribi, H. Belhouchette, M. J. Escorihuela, and V. Demarez. 2019. Mapping irrigated areas using sentinel-1 time series in Catalonia, Spain. *Remote Sensing* 11, 15 (2019), 25. https://www.mdpi.com/2072-4292/11/15/1836

[4] D. Bjorneberg, B. King, and A. Koehn. 2020. Watershed water balance changes as furrow irrigation is converted to sprinkler irrigation in an arid region. *Journal of Soil and Water Conservation* 75, 3 (2020), 254–262. doi:10.2489/jswc.75.3.254

[5] S Bontemps, M Boettcher, C Brockmann, G Kirches, C Lamarche, J Radoux, M Santoro, E Vanbogaert, U Wegmüller, M Herold, et al. 2015. Multi-year global land cover mapping at 300 m and characterization for climate modelling: achievements of the Land Cover component of the ESA Climate Change Initiative. *The International Archives of the Photogrammetry, Remote Sensing and Spatial Information Sciences* 40 (2015), 323–328.

[6] Jesslyn F Brown and Md Shahriar Pervez. 2014. Merging remote sensing data and national agricultural statistics to model change in irrigated agriculture. *Agricultural Systems* 127 (2014), 28–40.

[7] Inacio T Bueno, João FG Antunes, Aliny A Dos Reis, João PS Werner, Ana PS-GDD Toro, Gleyce KDA Figueiredo, Júlio CDM Esquerdo, Rubens AC Lamparelli, Alexandre C Coutinho, and Paulo SG Magalhães. 2023. Mapping integrated crop-livestock systems in Brazil with planetscope time series and deep learning. *Remote Sensing of Environment* 299 (2023), 113886.

[8] Manuel Campos-Taberner, Francisco Javier García-Haro, Beatriz Martínez, Emma Izquierdo-Verdiguier, Clement Atzberger, Gustau Camps-Valls, and María Amparo Gilabert. 2020. Understanding deep learning in land use classification based on Sentinel-2 time series. *Scientific reports* 10, 1 (2020), 17188.

[9] L. Chen and M. Wang. 2022. Extracting Agricultural Fields from Remote Sensing Imagery Using Graph-Based Growing Contours. *Remote Sensing, MDPI* (2022). https://www.mdpi.com/2072-4292/12/7/1205

[10] Yezhen Cong, Samar Khanna, Chenlin Meng, Patrick Liu, Erik Rozi, Yutong He, Marshall Burke, David Lobell, and Stefano Ermon. 2022. Satmae: Pre-training transformers for temporal and multi-spectral satellite imagery. *Advances in Neural Information Processing Systems* 35 (2022), 197–211.

[11] Thijs de Geus, Panagiotis Meletis, and Gijs Dubbelman. 2020. Fast Panoptic Segmentation Network. *IEEE Robotics and Automation Letters* 1 (2020), 1–2, 6.

[12] Jillian M Deines, Anthony D Kendall, Morgan A Crowley, Jeremy Rapp, Jeffrey A Cardille, and David W Hyndman. 2019. Mapping three decades of annual irrigation across the US High Plains Aquifer using Landsat and Google Earth Engine. *Remote Sensing of Environment* 233 (2019), 111400.

[13] Caitlin Dempsey. 2024. Normalized Difference Water Index (NDWI) and Its Use in Flood Detection. Geography Realm. https://www.geographyrealm.com/normalized-difference-water-index-flooding/ Accessed: February 7, 2024.

[14] Maurilio Di Cicco, Ciro Potena, Giorgio Grisetti, and Alberto Pretto. 2017. Automatic model based dataset generation for fast and accurate crop and weeds detection. In *2017 IEEE/RSJ International Conference on Intelligent Robots and Systems (IROS)*. IEEE, 5188–5195.

[15] Petra Döll and Stefan Siebert. 2000. A digital global map of irrigated areas. *ICID J* 49, 2 (2000), 55–66.

[16] Ernest A Engelbert and Ann Foley Scheuring. 2023. *Water scarcity: Impacts on western agriculture.* Univ of California Press.

[17] Rachel R Fern, Elliott A Foxley, Andrea Bruno, and Michael L Morrison. 2018. Suitability of NDVI and OSAVI as estimators of green biomass and coverage in a semi-arid rangeland. *Ecological Indicators* 94 (2018), 16–21.

[18] Jonathan A Foley, Navin Ramankutty, Kate A Brauman, Emily S Cassidy, James S Gerber, Matt Johnston, Nathaniel D Mueller, Christine O'Connell, Deepak K Ray, Paul C West, et al. 2011. Solutions for a cultivated planet. *Nature* 478, 7369 (2011), 337–342.

[19] Bo-Cai Gao. 1996. NDWI—A normalized difference water index for remote sensing of vegetation liquid water from space. *Remote sensing of environment* 58, 3 (1996), 257–266.

[20] Anatoly A Gitelson. 2004. Wide dynamic range vegetation index for remote quantification of biophysical characteristics of vegetation. *Journal of plant physiology* 161, 2 (2004), 165–173.

[21] Abdurrahman Gonenc, Mehmet Sirac Ozerdem, and ACAR Emrullah. 2019. Comparison of NDVI and RVI vegetation indices using satellite images. In *2019 8th International Conference on Agro-Geoinformatics (Agro-Geoinformatics)*. IEEE, 1–4.

[22] Cassandra Handan-Nader and Daniel E Ho. 2019. Deep learning to map concentrated animal feeding operations. *Nature Sustainability* 2, 4 (2019), 298–306.

[23] Alfredo Huete, Kamel Didan, Tomoaki Miura, E Patricia Rodriguez, Xiang Gao, and Laerte G Ferreira. 2002. Overview of the radiometric and biophysical performance of the MODIS vegetation indices. *Remote sensing of environment* 83, 1-2 (2002), 195–213.

[24] Calvin Hung, Zhe Xu, and Salah Sukkarieh. 2014. Feature learning based approach for weed classification using high resolution aerial images from a digital camera mounted on a UAV. *Remote Sensing* 6, 12 (2014), 12037–12054.

[25] James A. Ippolito, Dave L. Bjorneberg, Steve W. Blecker, and Michael S. Massey. 2019. Mechanisms Responsible for Soil Phosphorus Availability Differences between Sprinkler and Furrow Irrigation. *Journal of Environmental Quality* 48, 5 (2019), 1370–1379. doi:10.2134/jeq2019.01.0016 arXiv:https://acsess.onlinelibrary.wiley.com/doi/pdf/10.2134/jeq2019.01.0016

[26] Johannes Jakubik, S Roy, CE Phillips, P Fraccaro, D Godwin, B Zadrozny, D Szwarcman, C Gomes, G Nyirjesy, B Edwards, et al. [n. d.]. Foundation models for generalist geospatial artificial intelligence, 2023. *URL https://arxiv. org/abs/2310.18660* ([n. d.]).

[27] Xiaowei Jia, Mengdie Wang, Ankush Khandelwal, Anuj Karpatne, and Vipin Kumar. 2019. Recurrent Generative Networks for Multi-Resolution Satellite Data: An Application in Cropland Monitoring. In *Proceedings of the Twenty-Eighth International Joint Conference on Artificial Intelligence (IJCAI-19)*. 2628–2634. doi:10.24963/ijcai.2019/365

[28] Zhenong Jin, George Azzari, Marshall Burke, Stephen Aston, and David B Lobell. 2017. Mapping smallholder yield heterogeneity at multiple scales in Eastern Africa. *Remote Sensing* 9, 9 (2017), 931.

[29] David Ketchum, Kelsey Jencso, Marco P Maneta, Forrest Melton, Matthew O Jones, and Justin Huntington. 2020. IrrMapper: A machine learning approach for high resolution mapping of irrigated agriculture across the Western US. *Remote Sensing* 12, 14 (2020), 2328.

[30] Nataliia Kussul, Mykola Lavreniuk, Sergii Skakun, and Andrii Shelestov. 2017. Deep learning classification of land cover and crop types using remote sensing data. *IEEE Geoscience and Remote Sensing Letters* 14, 5 (2017), 778–782.

[31] Billie Leff, Navin Ramankutty, and Jonathan A Foley. 2004. Geographic distribution of major crops across the world. *Global biogeochemical cycles* 18, 1 (2004).

[32] Guoyong Leng, L Ruby Leung, and Maoyi Huang. 2017. Significant impacts of irrigation water sources and methods on modeling irrigation effects in the ACME L and Model. *Journal of Advances in Modeling Earth Systems* 9, 3 (2017), 1665–1683.

[33] Licheng Liu, Shaoming Xu, Jinyun Tang, Kaiyu Guan, Timothy J Griffis, Matthew D Erickson, Alexander L Frie, Xiaowei Jia, Taegon Kim, Lee T Miller, et al. 2022. KGML-ag: a modeling framework of knowledge-guided machine learning to simulate agroecosystems: a case study of estimating N 2 O emission using data from mesocosm experiments. *Geoscientific model development* 15, 7 (2022), 2839–2858.

[34] Licheng Liu, Wang Zhou, Kaiyu Guan, Bin Peng, Shaoming Xu, Jinyun Tang, Qing Zhu, Jessica Till, Xiaowei Jia, Chongya Jiang, et al. 2024. Knowledge-guided machine learning can improve carbon cycle quantification in agroecosystems. *Nature communications* 15, 1 (2024), 357.

[35] Thomas R Loveland, Bradley C Reed, Jesslyn F Brown, Donald O Ohlen, Zhiliang Zhu, LWMJ Yang, and James W Merchant. 2000. Development of a global land cover characteristics database and IGBP DISCover from 1 km AVHRR data. *International journal of remote sensing* 21, 6-7 (2000), 1303–1330.

[36] Eric Marcon, Ivan Scotti, Bruno Hérault, Vivien Rossi, and Gabriel Lang. 2014. Generalization of the partitioning of Shannon diversity. *PloS one* 9, 3 (2014), e90289.

[37] Molly A Maupin. 2018. *Summary of estimated water use in the United States in 2015.* Technical Report. US Geological Survey.

[38] Jonas Meier, Florian Zabel, and Wolfram Mauser. 2018. A global approach to estimate irrigated areas–a comparison between different data and statistics. *Hydrology and Earth System Sciences* 22, 2 (2018), 1119–1133.

[39] S Meivel and SJMS Maheswari. 2022. Monitoring of potato crops based on multispectral image feature extraction with vegetation indices. *Multidimensional Systems and Signal Processing* 33, 2 (2022), 683–709.

[40] Andres Milioto, Philipp Lottes, and Cyrill Stachniss. 2017. Real-time blob-wise sugar beets vs weeds classification for monitoring fields using convolutional neural networks. *ISPRS Annals of the Photogrammetry, Remote Sensing and Spatial Information Sciences* 4 (2017), 41–48.

[41] Anders Krogh Mortensen, Mads Dyrmann, Henrik Karstoft, Rasmus Nyholm Jørgensen, and René Gislum. 2016. Semantic segmentation of mixed crops using deep convolutional neural network. (2016).

[42] Md Shahriar Pervez and Jesslyn F Brown. 2010. Mapping irrigated lands at 250-m scale by merging MODIS data and national agricultural statistics. *Remote Sensing* 2, 10 (2010), 2388–2412.

[43] IR-4 Project. 2012. Index of crops/crop groups/crop subgroups, and crop definitions. (2012).

[44] Shanto Rahman, Md Mostafijur Rahman, Mohammad Abdullah-Al-Wadud, Golam Dastegir Al-Quaderi, and Mohammad Shoyaib. 2016. An adaptive gamma correction for image enhancement. *EURASIP Journal on Image and Video Processing* 2016 (2016), 1–13.

[45] Hannah Ritchie and Max Roser. 2018. Water use and stress. *Our World in Data* (2018).

[46] M. L. Rodrigues, T. S. Korting, and G. R. de Queiroz. 2020. Circular hough transform and balanced random forest to detect center pivot systems. In *GeoInfo*. 106–117.

[47] J. M. Salmon, M. A. Friedl, S. Frolking, D. Wisser, and E. M. Douglas. 2015. Global rain-fed, irrigated, and paddy croplands: A new high resolution map derived from remote sensing, crop inventories and climate data. *International Journal of Applied Earth Observation and Geoinformation* 38 (2015), 321–334.

[48] M. Saraiva, E. Protas, M. Salgado, and C. Souza. 2020. Automatic mapping of center pivot irrigation systems from satellite images using deep learning. *Remote Sensing* 12, 3 (2020), 14. https://www.mdpi.com/2072-4292/12/3/558

[49] Stefan Siebert, Jacob Burke, Jean-Marc Faures, Karen Frenken, Jippe Hoogeveen, Petra Döll, and Felix Theodor Portmann. 2010. Groundwater use for irrigation–a global inventory. *Hydrology and earth system sciences* 14, 10 (2010), 1863–1880.

[50] Stefan Siebert, Petra Döll, Jippe Hoogeveen, J-M Faures, Karen Frenken, and Sebastian Feick. 2005. Development and validation of the global map of irrigation areas. *Hydrology and Earth System Sciences* 9, 5 (2005), 535–547.

[51] Stefan Siebert, Verena Henrich, Karen Frenken, and Jacob Burke. 2013. Update of the digital global map of irrigation areas to version 5. *Rheinische Friedrich-Wilhelms-Universität, Bonn, Germany and Food and Agriculture Organization of the United Nations, Rome, Italy* 10, 2.1 (2013), 2660–6728.

[52] S. Siebert, M. Kummu, M. Porkka, P. Doll, N. Ramankutty, and B. R. Scanlon. 2015. A global data set of the extent of irrigated land from 1900 to 2005. *Hydrology and Earth System Sciences* 19, 3 (2015), 1521–1545.

[53] S. Siebert, M. Kummu, M. Porkka, P. Döll, N. Ramankutty, and B. R. Scanlon. 2015. A global data set of the extent of irrigated land from 1900 to 2005. *Hydrology and Earth System Sciences* 19, 3 (2015), 1521–1545. doi:10.5194/hess-19-1521-2015

[54] James A Slater and Stephen Malys. 1998. Wgs 84—past, present and future. In *Advances in Positioning and Reference Frames: IAG Scientific Assembly Rio de Janeiro, Brazil, September 3–9, 1997*. Springer, 1–7.

[55] Michael J Smith, Luke Fleming, and James E Geach. 2023. EarthPT: a foundation model for Earth Observation. *arXiv preprint arXiv:2309.07207* (2023).

[56] Pardhasaradhi Teluguntla, Prasad S Thenkabail, Jun Xiong, Murali Krishna Gumma, Chandra Giri, Cristina Milesi, Mutlu Ozdogan, Russ Congalton, James Tilton, Temuulen Tsagaan Sankey, et al. 2015. Global Cropland Area Database (GCAD) derived from remote sensing in support of food security in the twenty-first century: current achievements and future possibilities. (2015).

[57] Prasad S Thenkabail, Chandrashekhar M Biradar, Praveen Noojipady, Venkateswarlu Dheeravath, Yuanjie Li, Manohar Velpuri, Muralikrishna Gumma, Obi Reddy P Gangalakunta, Hugh Turral, Xueliang Cai, et al. 2009. Global irrigated area map (GIAM), derived from remote sensing, for the end of the last millennium. *International journal of remote sensing* 30, 14 (2009), 3679–3733.

[58] Franck Thénot, Maurice Méthy, and Thierry Winkel. 2002. The Photochemical Reflectance Index (PRI) as a water-stress index. *International Journal of Remote Sensing* 23, 23 (2002), 5135–5139.

[59] Compton J Tucker. 1985. Satellite remote sensing of total herbaceous biomass production in the Senegalese Sahel: 1980–1984. *Remote sensing of environment* 17, 3 (1985), 233–249.

[60] UN Water. 2020. The United Nations World Water Development Report 2020 Water and Climate Change (p. 235). United Nations educational.

[61] Marie Weiss, Frédéric Jacob, and Grgory Duveiller. 2020. Remote sensing for agricultural applications: A meta-review. *Remote sensing of environment* 236 (2020), 111402.

[62] Yanhua Xie, Holly K Gibbs, and Tyler J Lark. 2021. Landsat-based Irrigation Dataset (LANID): 30 m resolution maps of irrigation distribution, frequency, and change for the US, 1997–2017. *Earth System Science Data* 13, 12 (2021), 5689–5710.

[63] Kun Zhang, Xin Li, Donghai Zheng, Ling Zhang, and Gaofeng Zhu. 2022. Estimation of global irrigation water use by the integration of multiple satellite observations. *Water Resources Research* 58, 3 (2022), e2021WR030031.

[64] X. Zhang and Y. Lee. 2023. Deriving Agricultural Field Boundaries for Crop Management from Satellite Images Using Semantic Feature Pyramid Network. *Remote Sensing, MDPI* (2023). https://www.mdpi.com/2072-4292/15/11/2937

[65] Baojuan Zheng, James B Campbell, and Kirsten M de Beurs. 2014. Remote sensing of crop residue cover using multi-temporal Landsat imagery. *Remote Sensing of Environment* 156 (2014), 312–321.

Supplementary Material

A Properties of datasets

Table 6: Summary of total storage size for LandSat and Sentinel per state and year. Sizes are given in GB or TB where appropriate.

State	Year	LandSat Size (GB/TB)	Sentinel Size (GB/TB)
AZ	2013	78 GB	
	2014	116 GB	
	2015	94 GB	42 GB
	2016	117 GB	355 GB
	2017	133 GB	447 GB
CO	2018	86 GB	350 GB
	2019	65 GB	352 GB
	2020	88 GB	629 GB
UT	2021	72 GB	501 GB
	2022	129 GB	662 GB
	2023	117 GB	435 GB
WA	2015	45 GB	1 GB
	2016	53 GB	83 GB
	2017	51 GB	176 GB
	2018	45 GB	266 GB
	2019	37 GB	188 GB
	2020	47 GB	312 GB
Total		**1.4 TB**	**4.8 TB**

B Data Analysis

We analyze the diversity of the irrigation practices within the patches for each studied state. We notice that each state has a significant number of homogeneous patches (Shannon-index equal to 0) as shown in Figure 5. However, for Utah and Colorado, the distribution of shannon-index has a higher number of patches for the second peak (shannon-index equal to 0.7) compared to Arizona and Washington. Moreover, the numbers of heterogeneous patches are larger in Colorado and Utah compared to Arizona and Washington, indicating mixed irrigation practices in these two states.

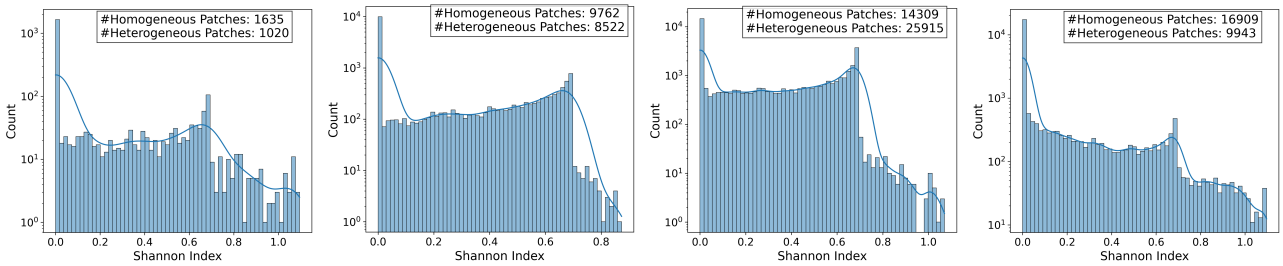

(a) Arizona **(b) Colorado** **(c) Utah** **(d) Washington**

Figure 5: The figure shows diversity of irrigation patterns across the states through Shannon diversity indices. Figure (a) presents Arizona's distribution; Figure (b) illustrates Colorado's similar pattern of irrigation concentration, with most patches having a Shannon index = 0.0; Figure (c) displays Utah's irrigation diversity, whereas Figure (d) shows Washington's irrigation diversity within patches.

C Evaluation Metrics

We evaluate the irrigation mapping task using four standard segmentation metrics: Intersection over Union (IoU), Precision (P), Recall (R), and F1-Score (F1). Let Y and $\overline{Y}$ be the ground truth and predicted masks, respectively, for an image of size $H \times W$, where each pixel (i, j) is assigned a class $k \in \mathcal{Y}$. The ground truth and predicted pixel sets for class k are defined as:

$$T_k = \{(i, j) \mid Y_{i,j} = k\}, \quad M_k = \{(i, j) \mid \overline{Y}_{i,j} = k\}. \tag{2}$$

The evaluation metrics precision, recall, F1, and IoU are computed as:

$$\mathrm{P}_k = \frac{|M_k \cap T_k|}{|M_k|}, \qquad \mathrm{R}_k = \frac{|M_k \cap T_k|}{|T_k|}, \qquad \mathrm{F1}_k = \frac{2 \times P_k \times R_k}{P_k + R_k}, \qquad \mathrm{IoU}_k = \frac{|M_k \cap T_k|}{|M_k \cup T_k|}, \tag{3}$$

Precision measures the proportion of correctly predicted irrigated pixels among all predicted as class k, while recall quantifies the fraction of correctly identified irrigated pixels out of all actual class k pixels. On the contrary, F1-Score computes the harmonic mean of precision and recall. IoU is defined as the ratio of intersection to union, provides a more balanced spatial evaluation by penalizing both over-segmentation (false positives) and under-segmentation (false negatives).

D Benchmarking

Parameter Settings. Hyperparameter details for supervised experiments can be seen in Table 7. We did not perform significant hyperparameter tuning. Model selection was based on the best performance on the validation set.

Additional Experiments. In Table 8, we present the overall performance on the training set. For training on Sentinel data, we use the same hyper-parameters and model architecture as Landsat. We randomly sample 100K training and test data from the IrrMap Sentinel dataset and train the model for five epochs.

The results indicate that the inclusion of additional bands, such as crop type and NDVI, has a notable impact on irrigation classification performance for both LandSat and Sentinel datasets. In LandSat, the RGB+CROP modality consistently outperforms other configurations, particularly in Flood and Sprinkler irrigation, suggesting that crop type information significantly enhances classification accuracy. Similarly, RGB+NDVI improves performance compared to standard RGB, but it does not surpass RGB+CROP, highlighting the greater influence of crop data over vegetation indices in LandSat imagery. For Sentinel, the impact of additional bands is even more pronounced, with RGB+CROP achieving the highest F1-scores and IoU across all irrigation methods, particularly for Sprinkler and Drip irrigation, where detailed crop information enhances model differentiation. RGB+LAND has also shown similar impact. The RGB+NDVI configuration also improves performance, especially in Sprinkler irrigation, reinforcing the value of vegetation indices at Sentinel's higher resolution. Overall, the inclusion of auxiliary bands positively influences classification performance, with crop type data playing a critical role in both datasets.

Table 7: Hyperparameter details for supervised ESAWC experiments

	Parameters
Task Type	Irrigation Method Segmentation
Loss Function	Cross Entropy
Input Dimensions	224×224
Input Channels: RGB	3
Input Channels:RGB+CROP	24
Input Channels: RGB+LAND	4
Input Channels: RGB+NDVI	4
Output Dimensions	224×224
Output Channels	4
Optimizer	Adam
Learning Rate	1.00×10^{-2}
No. Epochs (Landsat)	10
No. Epochs (Sentinel)	5
Model Selection	Best (val)
Framework	Pytorch Lightening

Table 8: Irrigation Classification Performance for Different Modalities, reporting Precision (P), Recall (R), F1-score (F), and Intersection over Union (IoU) for Flood, Sprinkler, and Drip irrigation methods across LandSat and Sentinel data.

Satellite	Modality	Flood				Sprinkler				Drip			
		P	R	F	IoU	P	R	F	IoU	P	R	F	IoU
LandSat	RGB	0.6080	0.2794	0.3829	0.2368	0.5666	0.4540	0.5041	0.3369	0.4133	0.3322	0.4145	0.2614
	RGB+CROP	**0.6821**	**0.6484**	**0.6648**	**0.4979**	**0.7176**	**0.7236**	**0.7206**	**0.5633**	0.5166	**0.5100**	**0.5133**	**0.3452**
	RGB+LAND	0.6671	0.5922	0.6274	0.4571	0.6857	0.6661	0.6758	0.5103	**0.5509**	0.3322	0.4145	0.2614
	RGB+NDVI	0.5685	0.4047	0.4728	0.3096	0.6058	0.4224	0.4977	0.3313	0.4360	0.1629	0.2372	0.1346
Sentinel	RGB	0.5497	0.4649	0.5038	0.3367	0.7488	0.6028	0.6679	0.5014	0.5775	0.0283	0.0539	0.0277
	RGB+CROP	**0.7259**	**0.6942**	**0.7097**	**0.5500**	**0.8061**	**0.8290**	**0.8174**	**0.6911**	0.5675	**0.6558**	**0.6085**	**0.4373**
	RGB+LAND	0.6861	0.6449	0.6649	0.4980	0.7947	0.7547	0.7742	0.6316	**0.5926**	0.3936	0.4731	0.3098
	RGB+NDVI	0.6172	0.4137	0.4954	0.3292	0.7252	0.6879	0.7061	0.5457	0.4827	0.2039	0.2867	0.1673

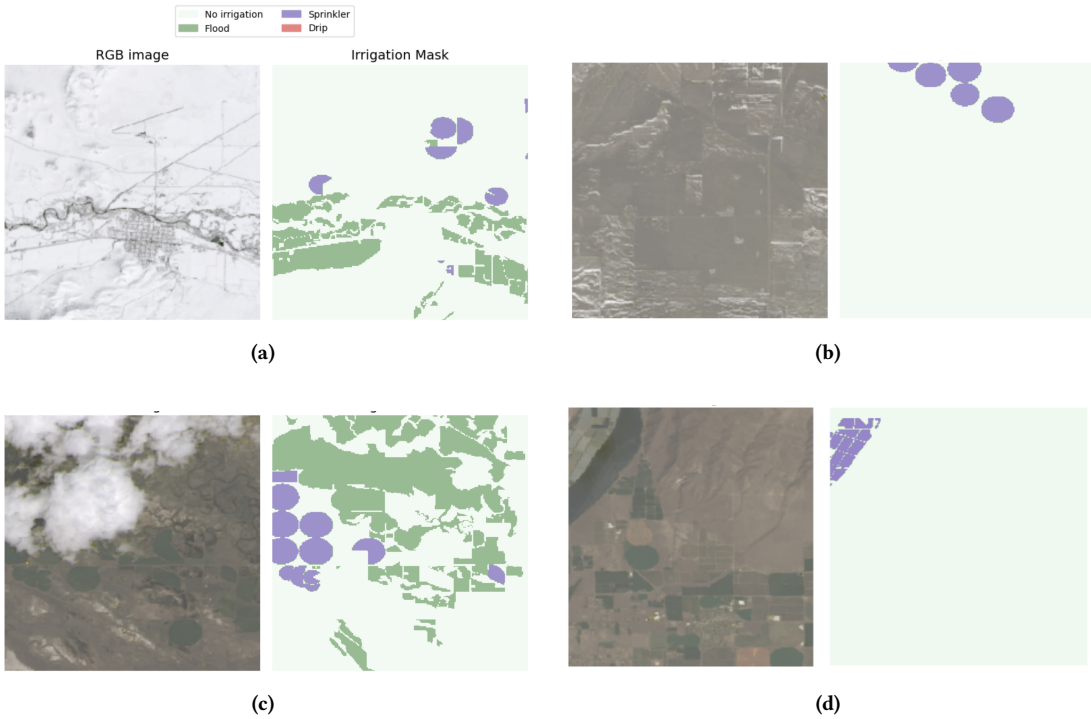

Figure 6: For each figure, the left image shows RGB images collected from satellite data, and the right figure shows the corresponding irrigation mask. (a) Agricultural land occluded by snow coverage, making irrigation methods identification difficult; (b) Poor image quality combined with snow coverage affecting landscape visibility; (c) Cloud and shadow occlusion impacting field visibility; and (d) Incomplete irrigation mask annotations with missing labels in the bottom region.

Table 9: Summary of Common Vegetation Indices, Their Purpose, and Use Cases

Index	Formula	Purpose	Common Use Cases
NDVI (Normalized Difference Vegetation Index)	$\frac{(NIR-Red)}{(NIR+Red)}$	Measures vegetation greenness and health	Crop monitoring, land cover classification, drought detection
EVI (Enhanced Vegetation Index)	$G \times \frac{(NIR-Red)}{(NIR+C_1 \times Red - C_2 \times Blue + L)}$	Reduces atmospheric and soil background effects	More sensitive to high biomass regions
GNDVI (Green Normalized Difference Vegetation Index)	$\frac{(NIR-Green)}{(NIR+Green)}$	More sensitive to chlorophyll content than NDVI	Water stress detection, photosynthetic activity
SAVI (Soil-Adjusted Vegetation Index)	$\frac{(NIR-Red)}{(NIR+Red+L)} \times (1+L)$	Minimizes soil background influence	Vegetation monitoring in arid or semi-arid areas
MSAVI (Modified Soil-Adjusted Vegetation Index)	$\frac{2NIR+1-\sqrt{(2NIR+1)^2-8(NIR-Red)}}{2}$	Further reduces soil influence compared to SAVI	Useful for sparse vegetation and dry land monitoring
RVI (Ratio Vegetation Index)	$\frac{NIR}{Red}$	Alternative to NDVI, less sensitive to atmospheric conditions	Biomass and vegetation density analysis
CIgreen (Chlorophyll Index)	$\frac{NIR}{Green} - 1$	Estimates chlorophyll content	Plant health monitoring
NDWI (Normalized Difference Water Index)	$\frac{(NIR-SWIR)}{(NIR+SWIR)}$	Measures water content in vegetation	Drought monitoring, irrigation management
PRI (Photochemical Reflectance Index)	$\frac{(Green-Blue)}{(Green+Blue)}$	Measures plant stress and efficiency	Photosynthesis monitoring
OSAVI (Optimized Soil-Adjusted Vegetation Index)	$\frac{(NIR-Red)}{(NIR+Red+0.16)}$	An improved version of SAVI that minimizes soil background effects while maintaining sensitivity to vegetation.	Used for vegetation monitoring in areas with moderate soil exposure.
WDRVI (Wide Dynamic Range Vegetation Index)	$\frac{a \times NIR-Red}{a \times NIR+Red}$	A modified NDVI that enhances sensitivity to vegetation changes in high biomass areas.	Used in precision agriculture to track crop growth and stress detection.
NDTI (Normalized Difference Tillage Index)	$\frac{(SWIR1-SWIR2)}{(SWIR1+SWIR2)}$	Differentiates between tilled and untilled soil, helping in soil disturbance and land management analysis.	Applied in soil erosion studies and land conservation planning.

Table 10: Mapping of Individual Crops to Crop Groups. The 'UNK' crop group indicates the crops can not be specified in any crop groups.

Crop Group	Individual Crops
Alfalfa	Alfalfa, Alfalfa/Barley Mix, Alfalfa/Grass, New Alfalfa
Cereals	Barley, Barley/Wheat, Cereal Grain, Corn, Durum Wheat, Grain/Seeds unspecified, Oats, Rye, Sorghum, Speltz, Spring Wheat, Triticale, Wheat, Winter Wheat, Corn Grain, Corn Silage, Small Grains, Sorghum Grain, Spring Grain, Sweet Corn, Wheat Fall, Wheat Spring, Field Corn, Double crop barley/corn, Double crop winter wheat/corn
Cover Crop	Cover Crop, Green Manure, Field Crops, Other Field Crops
Fibres	Cotton
Fruits	Apples, Apricots, Berries, Berry, Cherries, Citrus, Dates, Fruit Trees, Grapes, Melon, Oranges, Peaches, Pomegranate, Citrus Groves, Fruit
Grass	Bermuda Grass, Grass, Grass Hay, Hay/Silage, Idle Pasture, Other Hay/Non Alfalfa, Pasture, Pecan/Grass, Sod, Turfgrass, Turfgrass Ag, Turfgrass Urban, Grass Pasture, Bluegrass, Sod Farm, Grass/Hay/Pasture, Hay, Improved Pasture - Irrigated, Rye Grass, Grassland/Pasture, Irrigated turf
Green House	Greenhouse
Herb Group	Flowers, Herb
Horticulture	Horticulture
Nursery	Nurseries, Nursery, Nursery Trees, Tree Nurseries, Tree Nursery
Nuts	Almond, Pecans, Pistachios, Walnuts
Oil-bearing crops	Canola, Flaxseed, Jojoba, Mustard, OilSeed, Olives, Safflower, Soybeans
Orchard	Orchard, Orchard unspecified, Orchard With Cover, Orchard Wo Cover
Pulses	Beans, Dry Beans, Garbanzo, Seed, Peanuts, Seeds
Roots and Tubers	Potato, Potatoes
Shrub Plants	Guayule, Shrubland
Sugar Crops	Sugar Beets, Sugarbeets, Sunflower, Sugar Cane, Sugar cane
UNK	Commercial Tree, Fallow, Fallow/Idle, Field Crop unspecified, Idle, Not Specified, Other, Sudan, Transition, Trees, Urban, Ornamentals, Research Facility, Research land, Miscellaneous vegetables and fruits, Other tree crops
Vegetables	Flower Bulb, Lettuce, Onion, Pumpkins, Squash, Vegetable, Vegetables, Watermelons, Eggplant, Fall Vegetables, Spring Vegetables, Vegetables Double Crop, Cabbage, Onions, Peppers
Vineyard	Vineyard